Micromechanically based Finite Element Analyses of Composite Structures

A. Matzenmiller, S. Gerlach and B. Köster

University of Kassel, Institute of Mechanics, Mönchebergstr. 7, 34109 Kassel

1 Introduction

The numerical solution of boundary value problems in the field of composite structures requires the knowledge of the effective properties of the homogenised medium. The behaviour of composites can be described theoretically by means of continuum mechanics, based on a phenomenological approach. Micromechanical methods allow to predict the overall material behaviour of a representative volume element (RVE) analytically, if the properties and volume fractions of the different phases are given. In the present paper the micromechanical approach, known as the generalised method of cells (GMC), is used to model the microstructure of unidirectionally reinforced composite materials. The original method of cells (MOC) was developed by Aboudi (1991) to approximate the effective material properties. It can be applied to elastic as well as viscoelastic materials, see e.g. Matzenmiller & Gerlach (2004) and Gerlach & Matzenmiller (2002). Furthermore the GMC allows to consider the influence of the fibre-matrix-bond on the effective properties. The cohesive zone of fibres and matrix can be modelled either as a third material phase within the composite or as a two-dimensional interface. The present paper deals with the implementation of the nonlinear interface model, given by Needleman (1987), into the cells model. Thereby, a total decohesion of the fibres from the matrix can be modelled. Hence, it is possible to describe the softening material behaviour, which can be observed during the loading process of composite structures. The GMC algorithm is run simultaneously to the finite element analyses of the macrostructures.

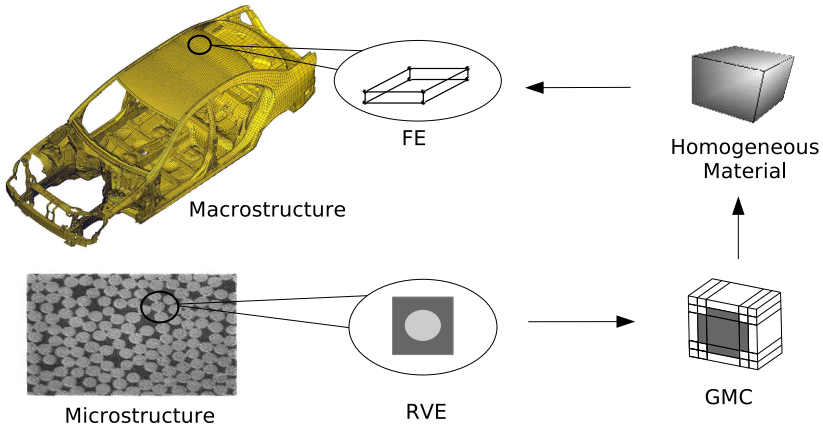

Figure 1.1: *Twoscale modelling in micromechanically based structural analyses.*

2 Micromechanically based modelling of composites

The intention of a microscopic view on inhomogeneous media is the analytical determination of the effective, averaged material properties of an equivalent, homogeneous surrogate material, based on the properties of the components and their volume fractions.The micromechanical modelling of composites is founded on the concept of a representative volume element (RVE). The RVE is defined as a part of the medium, which is structurally typical for the whole of the composite. Therefore, it should be large compared to the microstructure and small compared to the macrostructure. The averaged properties

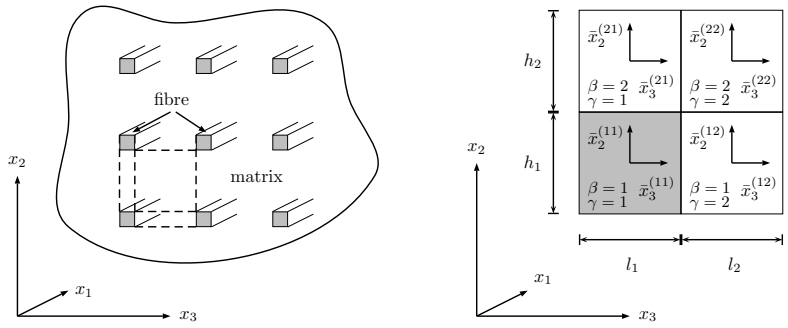

Figure 2.2: *Left: unidirectionally reinforced composite; assumption of double periodically arranged fibres. Right: RVE of the cells model consisting of four subcells.*

of the homogenised material are then defined by the effective stiffness tensor $\mathbb{C}^*$, which maps by its definition the volume averaged composite strains $\langle \boldsymbol{\epsilon} \rangle$ to the volume averaged composite stresses $\langle \boldsymbol{\sigma} \rangle$:

$$\langle \boldsymbol{\sigma} \rangle = \mathbb{C}^* \, : \langle \boldsymbol{\epsilon} \rangle, \tag{2.1}$$

which are calculated from

$$\langle \boldsymbol{\sigma} \rangle = \frac{1}{V} \int\limits_{\mathsf{RVE}} \boldsymbol{\sigma} \, \mathrm{d}V \quad \text{and} \quad \langle \boldsymbol{\epsilon} \rangle = \frac{1}{V} \int\limits_{\mathsf{RVE}} \boldsymbol{\epsilon} \, \mathrm{d}V. \tag{2.2}$$

Hence, the exact microscopic stress and strain fields $\boldsymbol{\sigma}$ and $\boldsymbol{\epsilon}$ must be known. By using micromechanical models, some simplifying assumptions are made to approximate the material properties of the composite closely. The introduction of Hill's averaged concentration tensors $\mathbb{A}^{(i)}$ constitutes an important basis of micromechanics.

$$\langle \boldsymbol{\epsilon}^{(i)} \rangle = \mathbb{A}^{(i)} : \langle \boldsymbol{\epsilon} \rangle \tag{2.3}$$

These concentration tensors map the average strains $\langle \boldsymbol{\epsilon} \rangle$ of the composite to the average strains $\langle \boldsymbol{\epsilon}^{(i)} \rangle$ of the phases i. By means of the stiffness tensors $\mathbb{C}^{(i)}$, which are assumed to be constant within each phase, the averaged stresses $\langle \boldsymbol{\sigma}^{(i)} \rangle$ of all components are given by the expression

$$\langle \boldsymbol{\sigma}^{(i)} \rangle = \mathbb{C}^{(i)} : \mathbb{A}^{(i)} : \langle \boldsymbol{\epsilon} \rangle. \tag{2.4}$$

Introducing the dimensionless volume fractions $c^{(i)} = V^{(i)}/V_{RVE}$ of the components, the average composite stress tensor $\langle \boldsymbol{\sigma} \rangle$ can be calculated from the weighted sum of the average cell stresses $\langle \boldsymbol{\sigma}^{(i)} \rangle$:

$$\langle \boldsymbol{\sigma} \rangle = \sum_i c^{(i)} \, \mathbb{C}^{(i)} : \mathbb{A}^{(i)} : \langle \boldsymbol{\epsilon} \rangle \quad \Rightarrow \quad \mathbb{C}^* := \sum_i c^{(i)} \, \mathbb{C}^{(i)} : \mathbb{A}^{(i)}. \tag{2.5}$$

Hence, the primary purpose of the micromechanical modelling is the determination of the concentration tensors $\mathbb{A}^{(i)}$, which are linking the averaged quantities on the macrolevel to those on the microlevel. The method of cells and its extension, the generalised method of cells (GMC), are approximate analytical methods for predicting the elastic as well as the inelastic responses of unidirectionally fibre-reinforced composites. The RVE of the GMC is given by the unitcell, depicted in Fig. 2. It is subdivided into $N_\beta \times N_\gamma$ rectangular subcells ($\beta\gamma$). The displacement field within each subcell is approximated by linear functions $u_i^{(\beta\gamma)}$ of the local coordinates $\bar{\mathbf{x}}^{(\beta\gamma)}$ and the microvariables $\phi_i^{(\beta\gamma)}$ and $\psi_i^{(\beta\gamma)}$.

$$u_i^{(\beta\gamma)} = w_i^{(\beta\gamma)} + \bar{x}_2^{(\beta)} \phi_i + \bar{x}_3^{(\gamma)} \psi_i \tag{2.6}$$

The quantities $w_i^{(\beta\gamma)}$ are describing the translations of the local coordinate systems $\bar{\mathbf{x}}^{(\beta\gamma)}$ attached to the subcells. By differentiating these displacement functions with respect to the local coordinates and

averaging the results over the subcell volumes, the average subcell strain vectors $\langle \boldsymbol{\epsilon}^{(\beta\gamma)} \rangle$ are received. Knowing the stiffness matrices $\mathbf{C}^{(\beta\gamma)}$ of the phases, the subcell stresses $\langle \boldsymbol{\sigma}^{(\beta\gamma)} \rangle$ can be calculated as well. The stress and displacement fields have to fullfill certain equilibrium and continuity conditions at the subcell interfaces, which lead to the following system of micromechanical equations:

$$\begin{array}{l} \text{continuity of displacements} \\ \text{equilibrium} \end{array} \qquad \underbrace{\left[\begin{array}{c} \mathbf{A}_{\mathsf{G}}(h_\beta, l_\gamma) \\ \hdashline \mathbf{A}_{\mathsf{M}}(C_{ik}^{(\beta\gamma)}) \end{array}\right]}_{\hat{\mathbf{A}}} \langle \boldsymbol{\epsilon}_s \rangle = \underbrace{\left[\begin{array}{c} \mathbf{J}(h,l) \\ \hdashline \mathbf{0} \end{array}\right]}_{\hat{\mathbf{J}}} \langle \boldsymbol{\epsilon} \rangle \tag{2.7}$$

The matrix $\mathbf{A}_{\mathsf{G}}$ depends on the geometry of the subcells, the stiffness matrices of the phases determine the matrix $\mathbf{A}_{\mathsf{M}}$. The total extensions h and l of the RVE enter the matrix $\mathbf{J}$. The vector $\langle \boldsymbol{\epsilon}_s \rangle$ contains the average strain vectors $\langle \boldsymbol{\epsilon}^{(\beta\gamma)} \rangle$ of all subcells $(\beta\gamma)$.
The solution of the system of equations (2.7) provides the desired concentration matrices $\mathbf{A}^{(\beta\gamma)}$, assembled in

$$\mathbf{A}^T = \left(\hat{\mathbf{A}}^{-1}\hat{\mathbf{J}}\right)^T = \left[\begin{array}{c|c|c|c} \mathbf{A}^{(11)} & \mathbf{A}^{(21)} & \ldots & \mathbf{A}^{(\beta\gamma)} \end{array}\right]. \tag{2.8}$$

Hence, the effective stiffness matrix $\mathbf{C}^*$ can be calculated, by using to the tensor equation (2.5).

$$\langle \boldsymbol{\sigma} \rangle = \mathbf{C}^* \langle \boldsymbol{\epsilon} \rangle \quad \Rightarrow \quad \mathbf{C}^* = \frac{1}{hl} \sum_{\beta=1}^{N_\beta} \sum_{\gamma=1}^{N_\gamma} h_\beta l_\gamma \mathbf{C}^{((\beta\gamma))} \mathbf{A}^{(\beta\gamma)} \tag{2.9}$$

3 Imperfect bond model

The GMC allows to take into account the imperfect bond of adjacent subcells. Therefore, the displacement continuity equations have to be modified. The displacement jumps $[\![u_i^{(\beta\gamma)}]\!]$ are introduced, which are defined as the differences of the displacement functions $u_i^{(\beta\gamma)}$ of the interface of adjacent subcells in an average sense. For interfaces with the normal vector $\mathbf{n}$ parallel to the global x_2-axis, this leads to:

$$[\![u_i^{(\beta\gamma)}]\!]_{\mathbf{n}\parallel\mathbf{e}_2} = \int_{-l_\gamma/2}^{l_\gamma/2} u_i^{(\hat{\beta}\gamma)}\big|_{\bar{x}_2^{(\hat{\beta})}=-h_{\hat{\beta}}/2} d\bar{x}_3^{(\gamma)} - \int_{-l_\gamma/2}^{l_\gamma/2} u_i^{(\beta\gamma)}\big|_{\bar{x}_2^{(\beta)}=h_\beta/2} d\bar{x}_3^{(\gamma)} \quad , \quad \hat{\beta} = \beta + 1 \tag{3.10}$$

and analogously for interfaces with the normal vector $\mathbf{n}$ pointing to the global direction x_3:

$$[\![u_i^{(\beta\gamma)}]\!]_{\mathbf{n}\parallel\mathbf{e}_3} = \int_{-l_\beta/2}^{l_\beta/2} u_i^{(\beta\hat{\gamma})}\big|_{\bar{x}_3^{(\hat{\gamma})}=-l_{\hat{\gamma}}/2} d\bar{x}_2^{(\beta)} - \int_{-h_\beta/2}^{h_\beta/2} u_i^{(\beta\gamma)}\big|_{\bar{x}_3^{(\gamma)}=l_\gamma/2} d\bar{x}_2^{(\beta)} \quad , \quad \hat{\gamma} = \gamma + 1. \tag{3.11}$$

Due to the bilinear displacement functions $u_i^{(\beta\gamma)}$, the magnitude of $[\![u_i^{(\beta\gamma)}]\!]$ is given by the difference of the displacements at the centres of the subcell surfaces, see Fig. 3.3. If all displacement jumps of all interfaces are listed in the vector $[\![\mathbf{u}]\!]_s$, the extended form of the system of micromechanical equations (2.7) can be written as:

$$\underbrace{\left[\begin{array}{c} \mathbf{A}_{\mathsf{G}}(h_\beta, l_\gamma) \\ \hdashline \mathbf{A}_{\mathsf{M}}(C_{ik}^{(\beta\gamma)}) \end{array}\right]}_{\hat{\mathbf{A}}} \langle \boldsymbol{\epsilon}_s \rangle + \underbrace{\left[\begin{array}{c} [\![\mathbf{u}]\!]_s \\ \hdashline \mathbf{0} \end{array}\right]}_{\mathbf{d}_s} = \underbrace{\left[\begin{array}{c} \mathbf{J}(h,l) \\ \hdashline \mathbf{0} \end{array}\right]}_{\hat{\mathbf{J}}} \langle \boldsymbol{\epsilon} \rangle. \tag{3.12}$$

Whereas the number of unknowns has been increased by introducing the displacement jumps $[\![\mathbf{u}]\!]_s$, the number of equations in (3.12) has remained unchanged. Therefore, additional equations are required to find a unique solution to the problem.

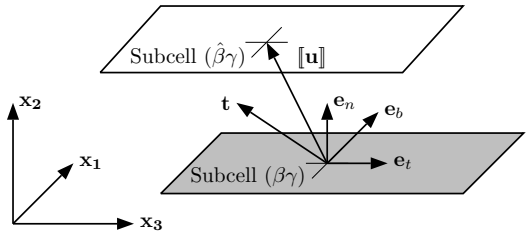

$$[\![\mathbf{u}]\!] = [\![u_n]\!]\,\mathbf{e}_n + [\![u_t]\!]\,\mathbf{e}_t + [\![u_b]\!]\,\mathbf{e}_b$$

$$\mathbf{t} = t_n\,\mathbf{e}_n + t_t\,\mathbf{e}_t + t_b\,\mathbf{e}_b$$

$$\hat{\beta} = \beta + 1$$

Figure 3.3: *Separation of adjacent subcells ($\hat{\beta}\gamma$) and ($\beta\gamma$): traction vector* $\mathbf{t}$*, displacement jump vector* $[\![\mathbf{u}]\!]$

3.1 Nonlinear interface model

The nonlinear interface model, proposed by Needleman (1987), provides three relations between the components of the interface traction vector $\mathbf{t}$ and the vector $[\![\mathbf{u}]\!]$ of the displacement jumps.

$$t_n = \frac{27}{4}\sigma_{max}\left[\frac{[\![u_n]\!]}{\delta}\left(1-\frac{[\![u_n]\!]}{\delta}\right)^2 + \alpha\left(\frac{[\![u_t]\!]}{\delta}\right)^2\left(\frac{[\![u_n]\!]}{\delta}-1\right) + \alpha\left(\frac{[\![u_b]\!]}{\delta}\right)^2\left(\frac{[\![u_n]\!]}{\delta}-1\right)\right] \tag{3.13}$$

$$t_t = \alpha\frac{27}{4}\sigma_{max}\left(1-\frac{[\![u_n]\!]}{\delta}\right)^2\frac{[\![u_t]\!]}{\delta} \qquad t_b = \alpha\frac{27}{4}\sigma_{max}\left(1-\frac{[\![u_n]\!]}{\delta}\right)^2\frac{[\![u_b]\!]}{\delta}$$

These equations hold for $[\![u_n]\!] \leq \delta$, wherein δ means a characteristic length. If $[\![u_n]\!]$ exceeds δ, all tractions will vanish identically, $\mathbf{t} \equiv \mathbf{0}$, except of the case with compression. σ_{max} is the maximum traction carried by the interface under purely normal separation and α specifies the ratio of shear to normal stiffness of the interface. The normal traction t_n increases with the normal separation $[\![u_n]\!]$ up to a stress maximum, then decreases to zero as complete fracture of the interface occurs, see Fig. 3.4 a). The dependence of the shear tractions t_t and t_b on the tangential displacements $[\![u_t]\!]$ and $[\![u_b]\!]$ is taken to be linear, while the tangential stiffnesses $S = S_t = S_b$ decrease nonlinearly with an increasing separation in normal direction.

$$S([\![u_n]\!]) := \alpha\frac{27}{4}\sigma_{max}\left(1-\frac{[\![u_n]\!]}{\delta}\right)^2 \tag{3.14}$$

The debonding model by Needleman does not take into account the influence of unloading or reloading processes in time τ on the interface behaviour. Therefore, the model is amended by introducing the internal variable q, defined as:

$$q := \begin{cases} \max\limits_{\tau\geq 0}([\![u_n]\!]/\delta) & \text{if} \quad 0 \leq [\![u_n]\!]/\delta \\ 1.0 & \text{if} \quad [\![u_n]\!] \geq \delta \end{cases} \tag{3.15}$$

By its definition in (3.15), the variable q measures and saves the maximum value of the normed displacement $[\![u_n]\!]/\delta$, attained during a strain controlled loading process in time τ. If the loading is reversed, $[\![u_n]\!]/\delta$ falls below q and the interface stress t_n is supposed to evolve linearly along the secant, indicated in Fig. 3.4 a). The coordinates of the traction vector $\mathbf{t}$ are then assumed as follows:

$$t_n = \frac{t_n(q)}{q}\,\frac{[\![u_n]\!]}{\delta} \qquad t_t = S_t(q)\,\frac{[\![u_b]\!]}{\delta} \qquad t_b = S_b(q)\,\frac{[\![u_b]\!]}{\delta} \tag{3.16}$$

Herein, t_n is given as a linear function of the normal displacement $0 \leq [\![u_n]\!]/\delta \leq q$, and a the constant slope of the secant, given by the quotient $t_n(q)/q$ of the normal stress $t_n(q)$, attained at the point of time when unloading begins, and the accompanying state of normal interface separation q. Otherwise, if no damage variable was considered, the stress t_n would increase although the displacement $[\![u_n]\!]$ decreased during unloading on the softening path. For decreasing $[\![u_n]\!]$ the tangential tractions are still linear functions of the tangential displacements, but the tangential stiffnesses $S = S(q) = const.$ do not change with $[\![u_n]\!]$. If $[\![u_n]\!]/\delta$ exceeds the former value of q within a possible reloading process, the stress displacement relations will again be given by the expressions (3.13).

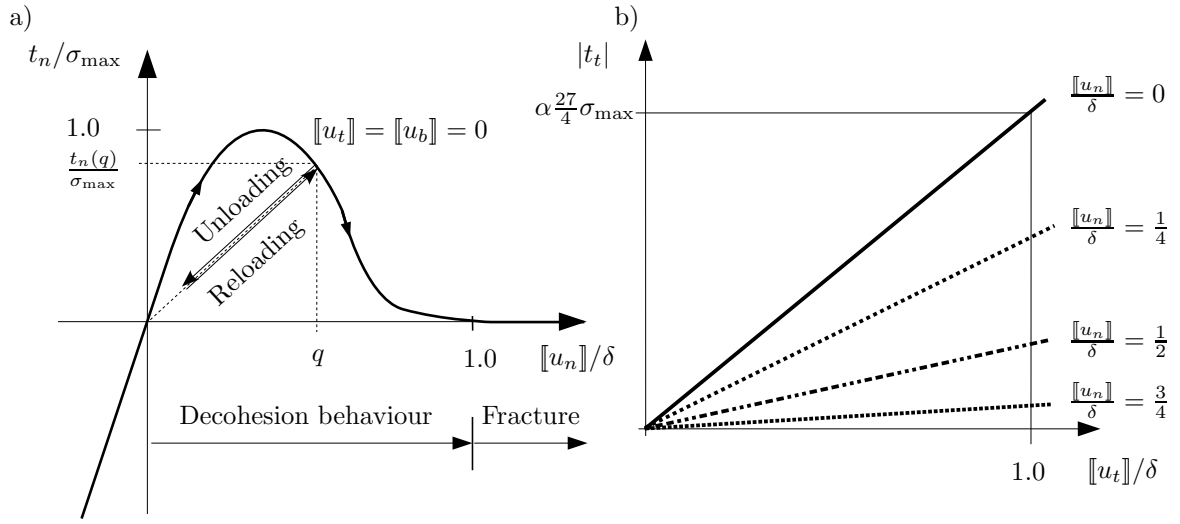

Figure 3.4: *a) Behaviour of the Needleman interface model under purely normal loading, ($[\![u_t]\!] = [\![u_b]\!] = 0$). b) Tangential stress displacement relations for various states of normal separations.*

Now the interface traction vector $\mathbf{t}$ can be regarded as a functional $\mathbf{f}([\![\mathbf{u}]\!], q)$ of the displacement jumps $[\![\mathbf{u}]\!]$ and the damage variable q. When it comes to the implementation of the interface model into the GMC-coding, the three equations for the components have to be formulated for all n fibre-matrix subcell interfaces I

$$\mathbf{t}^{(I)} = \mathbf{f}([\![\mathbf{u}^{(I)}]\!], q^{(I)}) \qquad I = 1, .., n. \tag{3.17}$$

These $n \times 3$ equations are assembled in the expression

$$\mathbf{t}_s = \mathbf{f}_s([\![\mathbf{u}]\!]_s, \mathbf{q}_s) \tag{3.18}$$

Combining (3.18) and (3.12), the system of micromechanical equations takes the implicit form:

$$\mathbf{R} = \begin{bmatrix} \mathbf{R}_1 \\ \mathbf{R}_2 \end{bmatrix} := \begin{bmatrix} \hat{\mathbf{A}}\langle\boldsymbol{\epsilon}_s\rangle + \mathbf{d}_s - \hat{\mathbf{J}}\langle\boldsymbol{\epsilon}\rangle \\ \mathbf{t_s} - \mathbf{f}_s([\![\mathbf{u}]\!]_s, \mathbf{q}_s) \end{bmatrix} = \begin{bmatrix} \mathbf{0} \\ \mathbf{0} \end{bmatrix}. \tag{3.19}$$

The incremental solution of the nonlinear system (3.19) can be found by applying iterative solution techniques such as arclength algorithms, see e.g. Schweizerhof (1989). When all subcell strains $\langle\boldsymbol{\epsilon}_s\rangle$ and displacement jumps $[\![\mathbf{u}]\!]_s$ have been calculated, the subcell strains can be expressed as a function of the composite strain and the displacement jumps, by rewriting the upper part of eq. (3.19):

$$\langle\boldsymbol{\epsilon}_s\rangle = \hat{\mathbf{A}}^{-1}\hat{\mathbf{J}}\langle\boldsymbol{\epsilon}\rangle - \hat{\mathbf{A}}^{-1}\mathbf{d}_s = \mathbf{A}\langle\boldsymbol{\epsilon}\rangle - \boldsymbol{\nu}, \tag{3.20}$$

with $\boldsymbol{\nu} := \hat{\mathbf{A}}^{-1}\mathbf{d}_s$ and $\mathbf{d}_s$ as defined in eq. (3.12). Hence, the subcell stresses are given by

$$\langle\boldsymbol{\sigma}^{(\beta\gamma)}\rangle = \mathbf{C}^{(\beta\gamma)}\langle\boldsymbol{\epsilon}^{(\beta\gamma)}\rangle \tag{3.21}$$

$$= \mathbf{C}^{(\beta\gamma)}\mathbf{A}^{(\beta\gamma)}\langle\boldsymbol{\epsilon}\rangle - \mathbf{C}^{(\beta\gamma)}\boldsymbol{\nu}^{(\beta\gamma)}. \tag{3.22}$$

The average composite stresses are decomposed into two parts:

$$\langle\boldsymbol{\sigma}\rangle = \langle\boldsymbol{\sigma}_{\mathsf{el}}\rangle - \langle\boldsymbol{\sigma}_{\mathsf{soft}}\rangle \tag{3.23}$$

The elastic part of the composite stress can be directly calculated from the composite strain $\langle\boldsymbol{\epsilon}\rangle$ by the concentration matrices $\mathbf{A}^{(\beta\gamma)}$

$$\langle\boldsymbol{\sigma}_{\mathsf{el}}\rangle = \frac{1}{hl}\sum_{\beta=1}^{N_\beta}\sum_{\gamma=1}^{N_\gamma} h_\beta l_\gamma \mathbf{C}^{(\beta\gamma)}\mathbf{A}^{(\beta\gamma)}\langle\boldsymbol{\epsilon}\rangle \tag{3.24}$$

The reduction of the composite stress due to the softening of the interface results in

$$\langle\boldsymbol{\sigma}_{\mathsf{soft}}\rangle = \frac{1}{hl}\sum_{\beta=1}^{N_\beta}\sum_{\gamma=1}^{N_\gamma} h_\beta l_\gamma \mathbf{C}^{(\beta\gamma)}\boldsymbol{\nu}^{(\beta\gamma)}. \tag{3.25}$$

4 Numerical examples

The effective stresses of a fibrous composite with imperfect bonding are plotted as functions of the overall strains in Fig. 4.5. During the fibre-matrix separation the effective stresses decrease as a function of growing effective strains. After separation only the matrix carries the effective stresses due to loading. The material properties are given in the following table.

Material and interface properties

Material	K-Modulus $[GPa]$	G-Modulus $[GPa]$	$v_f[\%]$	Ø-fibre μm
Glass	38.300	28.725	25	6.0
Epoxy	3.563	1.276	75	–
	$\sigma_{max}[MPa]$	$\alpha[-]$	$\delta\mu m$	
Interface	2.0	0.87	0.01 – 0.02	

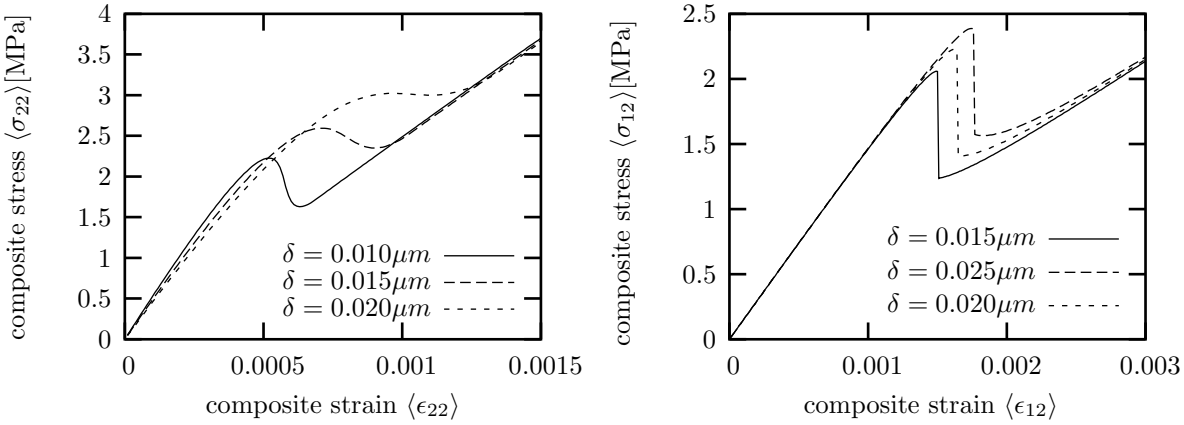

Figure 4.5: *Composite transverse and shear stresses vs. composite strains*

References

Aboudi, J. (1991). *Mechanics of composite materials - a unified micromechanical approach.* (1. ed.). Amsterdam: Elsevier.

Chaboche, J.L., R. Girad, A. Schaff (1997). Numerical analysis of composite systems by using interphase/interface models. *Computational Mechanics 20*, 3-11.

Gerlach, S. (2003). *Modellbildung und Parameteridentifikation viskoelastischer Faserverbundwerkstoffe.* Dissertation, Fachbereich Maschinenbau, Institut für Mechanik, Universität Kassel. URL: www.ifm.maschinenbau.uni-kassel.de/ifm/.

Gerlach, S. and Matzenmiller, A. (2002). Micromechanical Modeling of Viscoelastic Fiber-Matrix Bond in Composites, Proceedings of the Fifth World Congress on Computational Mechanics, July 2002, Eds.: Mang, H.A. etal., Vienna University of Technology, Austria.

Matzenmiller, A. and S. Gerlach (2001). Determination of effective material functions for linear viscoelastic fibrous composites with micromechanical model, Conference proceedings 'Trends in Computational Structural Mechanics'. Editors: W.A. Wall et al.. CIMNE, Barcelona, Spain 2001 .

Matzenmiller, A. and S. Gerlach (2004). Micromechanical modelling of viscoelastic composites with compliant fiber-matrix bonding. *Computational Materials Science 29*, 283–300.

Needlman, A. (1987). A Continuum Model for Void Nucleation by Inclusion Debonding. *Journal of Applied Mechanics 54*, 525–531.

Paley, M., Aboudi, J. (1992). Micromechanical analysis of composites by the generalized cells method. *Mechanics of Materials 14*, 127–139-

Schweizerhof, K. (1989). *Quasi-Newton Verfahren und Kurvenverfolgungsalgorithmen für die Lösung nichtlinearer Gleichungssysteme in der Strukturmechanik.* (Schriftenreihe Heft 9). Institut für Baustatik, Universität Fridericiana Karlsruhe.